

# Surface Characteristics of Spray-Dried Microspheres Consisting of PLGA and PVP: Relating the Influence of Heat and Humidity to the Thermal Characteristics of These Polymers

Joke Meeus,<sup>†</sup> David J. Scurr,<sup>‡</sup> Katie Amssoms,<sup>§</sup> Martyn C. Davies,<sup>‡</sup> Clive J. Roberts,<sup>‡</sup> and Guy Van den Mooter<sup>\*,†</sup>

<sup>†</sup>Drug Delivery and Disposition, KU Leuven, Belgium

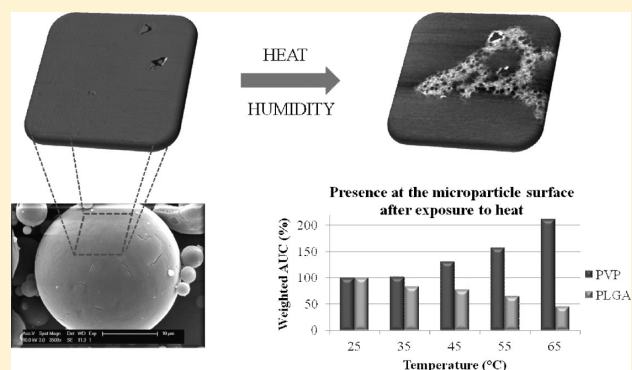
<sup>‡</sup>Laboratory of Biophysics and Surface Analysis, School of Pharmacy, The University of Nottingham, NG7 2RD, United Kingdom

<sup>§</sup>Pharmaceutical Companies of Johnson & Johnson, Janssen C.R.E.A.Te—Community of Research Excellence and Advanced Technology, Translational Sciences\_EDD, Beerse, Belgium

## S Supporting Information

**ABSTRACT:** In view of the increasing interest in injectable controlled release formulations for the treatment of chronic diseases, injectable polymeric microspheres consisting of a surface layer of poly(lactic-co-glycolic acid) (PLGA) and an underlying polyvinylpyrrolidone (PVP) layer were previously developed. The present study focuses on the influence of heat and humidity on the surface characteristics of these spray-dried PLGA/PVP microspheres. The response of the polymeric matrix to these factors will provide an insight into the expected release behavior and stability of the formulation. This should result in the development of a drug matrix with desired and tunable characteristics in terms of physicochemical stability and drug release profile, relevant in a later stage of research. Glass transition temperatures ( $T_g$ s) and miscibility behavior were analyzed by modulated differential scanning calorimetry (MDSC). Scanning electron microscopy (SEM) provided insight in particle morphology. Atomic force microscopy (AFM) was used to study the nanoscale topography and phase behavior of the samples. Time-of-flight secondary ion mass spectrometry (ToF-SIMS) and X-ray photoelectron spectroscopy (XPS) were utilized for surface chemical analysis and quantification respectively. It could be concluded that the surface characteristics (chemical composition, phase behavior, and topography) of spray-dried PVP/PLGA microparticles were affected by exposure to heat and humidity. When exposed to these conditions, a surface rearrangement occurs whereby an increase of PVP at the surface is observed, coupled with a decrease in PLGA. This phenomenon can be explained based upon the relative thermal characteristics and consequent molecular mobility of the two polymers.

**KEYWORDS:** surface analysis, microspheres, PLGA, PVP, MDSC, ToF-SIMS, parenteral controlled release, AFM, XPS



## INTRODUCTION

In view of the increasing interest in injectable controlled release formulations for the treatment of chronic diseases we aim to develop polymeric microspheres for intramuscular injection. The microspheres consist of two biocompatible polymers, particularly suitable for formulating poorly soluble drugs. For this matrix water insoluble poly(lactic-co-glycolic acid) (PLGA) is combined with water-soluble polyvinylpyrrolidone (PVP). The role of PLGA is to ensure the slow release characteristics of the formulation, whereas PVP is used to increase the solubility/dissolution rate of a poorly soluble active pharmaceutical ingredient (API) by forming a solid dispersion. To reach this goal, a phase separated system of these two polymers was pursued, in order to permit each polymer to accomplish its function.

Microspheres of these two polymers were prepared by spray drying. Previously an in-depth characterization of the surface characteristics and miscibility behavior of this system was performed.<sup>1</sup> This revealed that the shell structured, spray-dried microparticles consisted of a PLGA-rich surface layer and a PVP-rich underlying phase. These findings were supported by time-of-flight secondary ion mass spectrometry (ToF-SIMS), X-ray photoelectron spectroscopy (XPS), and nano thermal analysis (nanoTA) experiments.

In the present study, the influence of exposure to heat and humidity on the microparticle composition was investigated for

Received: May 2, 2013

Revised: July 3, 2013

Accepted: July 11, 2013

Published: July 11, 2013

a dual purpose. First, knowledge about the influence of humidity and temperature on the polymeric matrix is essential to gain insight into the shelf life/stability of the final formulation, which will be largely determined by the phase behavior of the matrix polymers. Furthermore exposing a formulation to stress conditions, such as heat and humidity, allows an accelerated study of the stability of this formulation.<sup>2–6</sup>

Second, the developed polymeric matrix is intended for controlled release injectable formulations implying that it will be in contact with human tissue for several weeks. This intramuscular environment implies an aqueous environment and to a lesser extent also elevated (body) temperatures. The response of the matrix to these factors will provide an insight into the expected drug release behavior of the formulation when injected into the intramuscular environment. This should result in the development of a drug matrix with desired and tunable characteristics in terms of physicochemical stability and drug release profile in a later stage of research.

Many contributions studying the influence of elevated temperatures and/or humidity on the bulk characteristics of a pharmaceutical sample have already been published.<sup>2–10</sup> In this study, special attention was paid to the influence of heat and humidity on the particle surface composition, in contrast to the bulk sample. This was motivated by the fact that the spray-dried particles are hollow microspheres with a relatively thin shell,<sup>1</sup> which implies that their surface comprises a significant part of the total sample mass. Hence a change in surface characteristics (for example due to exposure to heat and/or humidity) will significantly alter the bulk characteristics of the samples. Furthermore the microparticle surface will always be the first part of the formulation to come into contact with its (intramuscular) release environment.

Modulated differential scanning calorimetry (MDSC) was used to determine the glass transition temperatures ( $T_g$ ) of the pure polymers as well as the bulk miscibility behavior of the spray-dried samples. Scanning electron microscopy (SEM) provided insight in particle morphology. Atomic force microscopy (AFM) provided information about changes of the nanoscale phase behavior, induced by exposing the sample to an increased temperature or humidity. Chemical changes occurring at the sample surface were studied by means of the complementary techniques of ToF-SIMS and XPS.

This approach could be generalized and applied to other polymers as well by relating the thermal characteristics of the polymers used to the observations made after exposure of the samples to elevated temperature or humidity. Hence rationalization of our observations by elucidation of the underlying mechanism resulted in a generic approach, applicable to all polymers with known thermal characteristics.

The novelty of this study lies in the conception of the formulation surface as a determining and even the predicting factor for the bulk characteristics of that formulation. Furthermore a powerful combination of state-of-the-art techniques allows nanoscale surface characterization.

## ■ EXPERIMENTAL SECTION

**Materials.** Polyvinylpyrrolidone K30 (PVP K30) (MW 44–54 kDa) was kindly donated by BASF (Ludwigshafen, Germany). Poly(lactic-co-glycolic acid) (lactide:glycolide molar ratio of 75:25, inherent viscosity of 0.2 dL/g) was purchased from PURAC Biomaterials (Gorinchem, The Netherlands).

**Methods. Spray Drying.** Samples were prepared by spray drying with a Micro Spray lab scale spray dryer (ProCepT, Zelzate, Belgium). A 5% feed solution of the polymers in dichloromethane (DCM) was used. The inlet temperature was set to 115 °C, and the feed rate was 6 mL/min. The co-current drying air had a flow rate of 0.2 m<sup>3</sup>/min, and the atomizing air was supplied with a pressure of 1.25 bar.

**Temperature and Humidity Sample Pretreatment.** In order to investigate the influence of heat on the sample surface, a PLGA/PVP (40/60 wt %) sample was placed in an oven and exposed to a set of increasing temperatures (35, 45, 55, and 65 °C). Each sample was exposed to a specific temperature during 30 min at a relative humidity of a maximum of 30%. In addition, a variation in exposure time was made for the sample exposed to 65 °C (15, 22.5, 30, 37.5, and 45 min).

To investigate the influence of humidity a set of spray-dried PLGA/PVP (40/60 wt %) samples were exposed to increasing relative humidity (RH) (30, 40, 50, and 60%). Each sample was subjected to a specific RH during 30 min at room temperature. In addition a variation in exposure time was made for the sample exposed to RH 60% (15, 22.5, 30, 37.5, and 45 min). Relative humidities were set by using the sample chamber of an EnviroScope Atomic Force Microscope (BrukerNano, Coventry, UK).

**Modulated Differential Scanning Calorimetry.** MDSC (Q2000, TA Instruments, Leatherhead, U.K.) was used to determine the bulk miscibility behavior of the spray-dried microspheres. The data obtained were analyzed with the Thermal Analysis Software (Version 4.4A). Crimped aluminum pans (TA Instruments, Brussels, Belgium) were used for the analysis of the samples. An empty pan was used as a reference, and the masses of the reference pan and of the sample pans were taken into account. The DSC cell was purged with a nitrogen flow rate of 50 mL/min.

Temperature calibration was done using indium and octadecane. Calibration of the enthalpic response was performed with indium. The modulation parameters used were a heating rate of 1 °C/min, a period of 40 s, and an amplitude of 1 °C. Calibration of the heat capacity was done using sapphire. Samples were analyzed from –20 to 220 °C. Glass transitions were analyzed in the reversing heat flow signals.

**Scanning Electron Microscopy.** SEM was used to gain insight into the morphology and particle size of the samples. Samples were prepared by fixing an amount of powder on an aluminum stub using double-sided carbon tape. The samples were gold-coated by sputtering with gold for 45 s at 20 mA. Field emission gun scanning electron micrographs (FEG-SEM) were taken by using a Philips XL30 ESEM-FEG instrument (Philips, Eindhoven, The Netherlands) at an acceleration voltage of 10 kV.

**Atomic Force Microscopy.** An EnviroScope atomic force microscope was used for the AFM experiments. Measurements were conducted at a temperature of 25 °C and a relative humidity of 20%. Commercial silicon AFM tips were used (BrukerNano) with spring constants from 20 to 80 N m<sup>-1</sup> and resonance frequencies between 347 and 393 kHz. Mica slides (Agar Scientific, Stansted, U.K.) were used as sample substrate. Gwyddion software (version 2.22) was used for image analysis.

**Time-of-Flight Secondary Ion Mass Spectrometry.** Spray-dried samples were adhered to double-sided tape in order to produce an immobile surface suitable for ToF-SIMS analysis. The data were acquired using a ToF-SIMS IV instrument

(ION-TOF GmbH) equipped with a bismuth liquid metal ion gun and a single-stage reflectron analyzer. Typical operating conditions utilized a  $\text{Bi}_3^+$  primary ion energy of 25 kV and a pulsed target current of approximately 1.0 pA. A flood gun producing low energy electrons (20 eV) was used to compensate for surface charging caused by the positively charged primary ion beam on the insulating sample surface. A 4 mm  $\times$  4 mm area of each sample was raster scanned at a resolution of 600  $\times$  600 pixels, implying that each pixel has a size of 6.67  $\mu\text{m}$   $\times$  6.67  $\mu\text{m}$ . PLGA and PVP were identified using  $\text{C}_3\text{H}_3\text{O}_3^-$  ( $m/z = 87$ ), and the sum of  $\text{CN}^-$  ( $m/z = 26$ ) and  $\text{CNO}^-$  ( $m/z = 42$ ) respectively.<sup>1</sup> Prior to sample analysis, reference materials were analyzed and the characteristic peaks ( $\text{CN}^-$ ,  $\text{CNO}^-$ , and  $\text{C}_3\text{H}_3\text{O}_3^-$ ) were selected and only present in the appropriate samples. The secondary ion intensity for PVP and PLGA was mapped for each pixel. By keeping the total primary ion beam dose for every analyzed area below  $1 \times 10^{12}$  ions/ $\text{cm}^2$  throughout the analysis, static conditions were ensured. Data in the negative secondary ion polarities were collected and analyzed using SurfaceLab 6 (IONTOF). The imaged data were all acquired using the “high current bunched” setting on the instrument to achieve high mass resolution. For any given sample, the measured secondary ion intensity for each polymer marker peak was normalized to the total intensity count to enable a semiquantitative comparison of the different samples.

**X-ray Photoelectron Spectroscopy.** XPS analysis was performed using a Kratos Axis Ultra instrument (Kratos Analytic, Manchester, U.K.) equipped with a monochromated Al K $\alpha$  X-ray source (1486.6 eV), employing hybrid (magnetic/electrostatic) optics, a hemispherical analyzer, a multichannel plate, a delay line detector (DLD) with collection and takeoff angles of 30 and 90°, respectively. The instrument was operated at 15 mA emission current and 10 kV anode potential. Spray-dried samples were adhered to double-sided tape. Wide scans were run for 5–10 min at three different positions on the powder surface, with an analysis area of 0.3 mm  $\times$  0.7 mm. The instrument was run using the CASA XPS software (version 2.3.16). High energy resolution C 1s, N 1s, O 1s, and Si 2p spectra were obtained. Charge neutralization was accomplished during analysis using a flood gun.

Survey scans were accomplished using a pass energy of 80 eV, a step size of 1 eV, and an acquisition time of 10 min. High resolution scans were obtained using a pass energy of 20 eV, a step size of 0.1 eV, and an acquisition time of 5 min.

## RESULTS

**1. Influence of Heat and Humidity on the Bulk Miscibility of the Sample.** MDSC was used to thermally characterize the spray-dried polymers as well as the miscibility behavior of the spray-dried microspheres.

The amorphous spray-dried polymers were identified by their  $T_g$ s, being about 38 °C for PLGA and 172 °C for PVP respectively (under the given experimental conditions) (Figure 1A). MDSC was also utilized to study the bulk miscibility (and hence phase behavior) of the spray-dried sample (PLGA/PVP 40/60 wt %) through its glass transition temperatures, which were observed in the reversing heat flow curves (Figure 1A). For this sample, two  $T_g$ s were observed, demonstrating a phase separated system. The obtained  $T_g$  values do not correspond to the  $T_g$ s of the pure compounds but are shifted toward each other, suggesting two mixing  $T_g$ s.

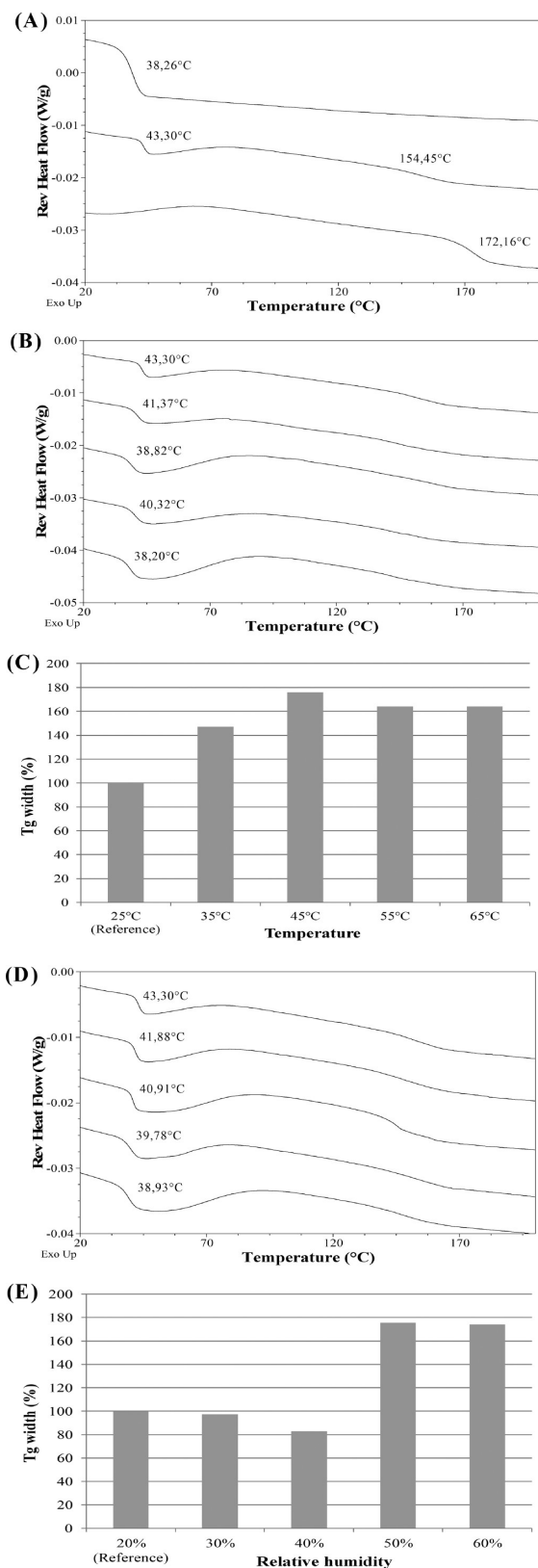


**Figure 1.** (A) MDSC of the pure spray-dried polymers and the reference sample. From top to bottom: reversing heat flow of PLGA, PLGA/PVP 40/60 wt % and PVP. (B) MDSC representing the influence of heat upon the value of the  $T_g$ . From top to bottom: reversing heat flow of a PLGA/PVP 40/60 wt % reference sample, a PLGA/PVP 40/60 wt % sample exposed to 35 °C, 45 °C, 55 °C, and 65 °C. (C) Histogram representing the influence of heat on the width

Figure 1. continued

of the  $T_g$  range of the PLGA phase. (D) MDSC representing the influence of humidity upon the value of the  $T_g$ . From top to bottom: reversing heat flow of a PLGA/PVP 40/60 wt % reference sample, a PLGA/PVP 40/60 wt % sample exposed to RH 30%, RH 40%, RH 50%, and RH 60%. (E) Histogram representing the influence of humidity on the width of the  $T_g$  range of the PLGA phase.

Based upon the mixing  $T_g$ s observed in the thermogram, the theoretical amounts of PVP present in the PLGA-rich phase (based upon  $T_{g1}$ , the first  $T_g$  observed in the thermograms) and of PLGA present in the PVP-rich phase (based upon  $T_{g2}$ , the second  $T_g$  observed in the thermograms) were estimated by means of the Gordon–Taylor equation (eq 1).

$$T_{g\text{mix}} = (w_1 T_{g1} + K w_2 T_{g2}) / (w_1 + K w_2) \quad (1)$$

In this equation, the weight fraction of each compound is represented by  $w$  and the glass transition by  $T_g$ , and the subscripts 1 and 2 represent the compounds with the lowest and the highest glass transition temperatures respectively. The constant  $K$  can be assessed by using the Simha–Boyer rule (eq 2), with  $\rho$  being the density of the amorphous compounds.

$$K \approx (\rho_1 T_{g1}) / (\rho_2 T_{g2}) \quad (2)$$

The PVP content in the PLGA phase was thus estimated to be 15% and the PLGA content in the PVP phase 3%. From this point onward these phases will be called the PLGA phase and the PVP phase, respectively.

In order to evaluate the influence of heat and humidity on the spray-dried microspheres not only were the observed temperature values for the  $T_g$ s brought into account but also the width of the  $T_g$  range was evaluated. The width of the  $T_g$  range provides information about the heterogeneity of the amorphous phase: the broader the  $T_g$  range, the more heterogeneous the amorphous phase.<sup>11–13</sup> It was preferred to study the PLGA phase (and hence broadening of that  $T_g$ ) instead of the PVP phase. The first reason for this choice is the fact that the PLGA phase is the surface layer of the spray-dried microspheres<sup>1</sup> and hence will be the first to be influenced by exposure to heat and humidity. Second, as seen in Figure 1A, the width of the  $T_g$  of the PLGA phase of the original sample (PLGA/PVP 40/60 wt %) is very narrow, indicating a homogeneous phase, which is a suitable start for evaluating the width of the  $T_g$  after exposure to heat/humidity. The  $T_g$  of the PLGA phase of samples subjected to heat or humidity is compared to the  $T_g$  of the PLGA phase of the original sample in Figure 1B–E.

For the study of the influence of exposure to heat, samples were subjected to elevated temperatures and the sample stored at room temperature (25 °C) was used as a reference. Analogously, for the study of the influence of exposure to humidity, samples were subjected to elevated relative humidity (RH) and the sample exposed to maximum 20% RH was used as reference sample. Figures 1B and 1D respectively show the influence of exposure to heat and humidity on the value of the  $T_g$  of the PLGA phase. It is observed that even the mildest conditions (exposure to 35 °C for heat, and a RH of 30% for humidity) result in a decrease of the  $T_g$  value, evolving from 43 °C down to 38 °C for both parameters.

Figure 1C displays the influence of exposure to heat onto the width of the  $T_g$  of the PLGA phase. The increase in width of the  $T_g$  was expressed as a percentage rise relative to the reference sample. It was observed for all samples for which exposure to heat resulted in a broadening of the  $T_g$ . This  $T_g$  broadening was 47% for samples exposed to 35 °C and went up to 76% for samples exposed to 45 °C.

A similar experiment was performed to study the influence of exposure to humidity on the width of the  $T_g$  and hence on the homogeneity of the amorphous PLGA surface layer. Upon exposure of the sample to a RH up to 40% no broadening of the  $T_g$  was observed, on the contrary for the latter the width of the  $T_g$  decreased with 17% (Figure 1E). However, when the samples were subjected to a RH of 50% or higher, the width of the  $T_g$  increased up to 76%.

## 2. Influence of Heat on the Sample Surface

**2.1. Influence of Heat on the Chemical Surface Composition.** The influence of elevated temperature on the chemical surface composition of the spray-dried microspheres was investigated by means of two complementary techniques. ToF-SIMS analysis provided information about the chemical composition of the first monolayers (1–2 nm) of the sample, based upon molecular fragmentation. XPS gathered information based upon the calculation of atomic concentrations, covering an increased sampling depth (ca. 10 nm).

**Time-of-Flight Secondary Ion Mass Spectrometry.** Spray-dried PLGA/PVP samples (40/60 wt %) were exposed to 35 °C, 45 °C, 55 °C, and 65 °C for 30 min in order to investigate the influence of elevated temperature on their chemical surface composition. SEM showed the particles to be roughly between 2 and 20  $\mu\text{m}$  in diameter (Figure 2). ToF-SIMS was used to analyze a 4 mm  $\times$  4 mm area covered with each sample. Taking into account the average particle size of the spray-dried material, this area contains a statistically representative number of particles. The ion intensity for PVP and PLGA was mapped and collected for each pixel in this area. A higher ion intensity

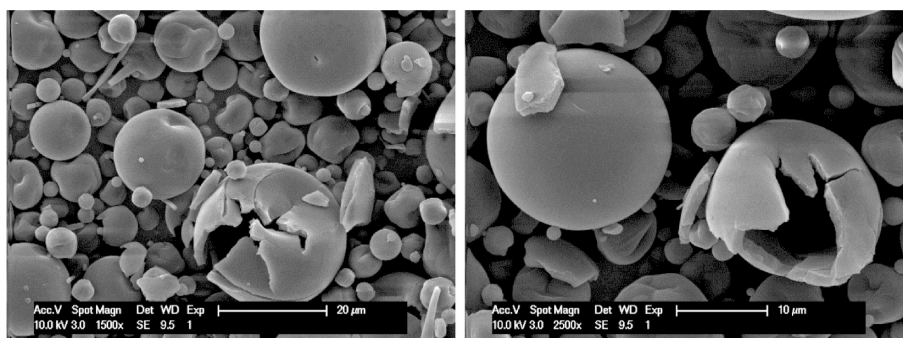
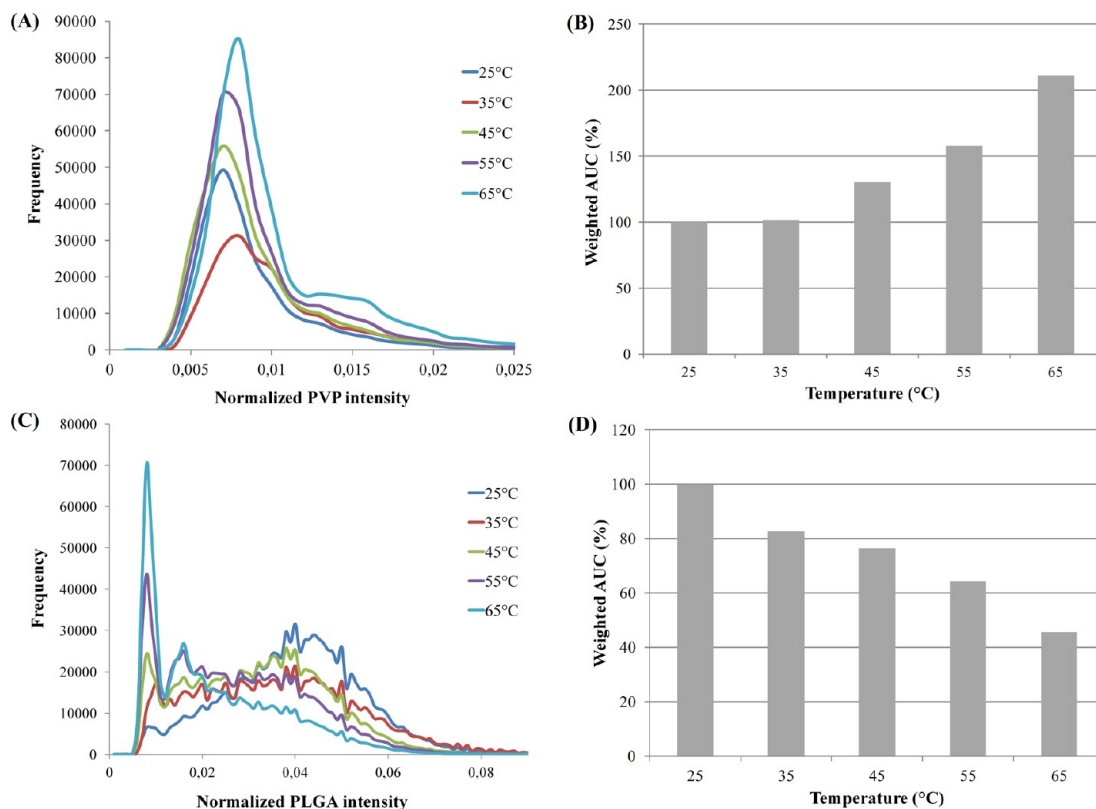
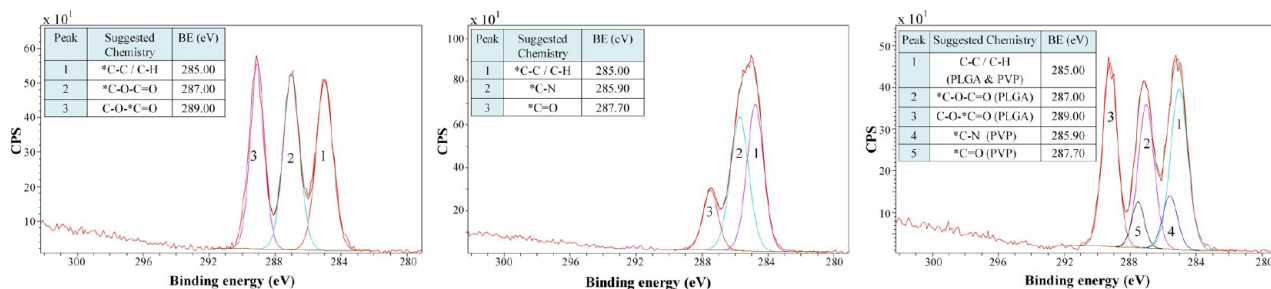


Figure 2. Scanning electron micrographs of a spray-dried reference sample, PLGA/PVP 40/60 wt %.



**Figure 3.** ToF-SIMS data. (A) Frequency distribution plot displaying the influence of heat upon the presence of PVP at the microsphere surface. (B) Weighted histogram representing the influence of heat upon the presence of PVP at the microsphere surface. (C) Frequency distribution plot displaying the influence of heat upon the presence of PLGA at the microsphere surface. (D) Weighted histogram representing the influence of heat upon the presence of PLGA at the microsphere surface.



**Figure 4.** XPS C 1s high resolution scans. Left to right: PLGA, PVP, and PLGA/PVP 40/60 wt %.

represents a larger amount of the compound present at that specific pixel. Hence, an overall increase in intensity signal of the examined 4 mm × 4 mm area can be related to two different underlying phenomena or a combination of both: a first possibility is an increased amount of the compound present at a constant surface coverage (increase in the amount of compound present at existing spots). The second option is an increase in the overall surface coverage of compound.

The results for PVP were plotted in a frequency distribution plot (FDP) (Figure 3A), which represents the pixel frequency of the different intensity levels for the scanned area. It should be emphasized that these FDPs were strictly qualitatively used to evaluate the influence of heat onto the sample surface. Figure 3A revealed that as the sample was exposed to elevated temperatures, there was a tendency of the respective frequency distribution plots to have an increased maximum height as well as augmented tailing at their right-hand side. The FDP for PLGA (Figure 3C) revealed a tendency opposite to that of

PVP: a shift of the FDP to the left with an increase in maximum height at the left-hand end.

Next, the AUC for each FDP was calculated, bringing into account not only the amount of pixels with a certain intensity level but also the magnitude of this intensity, resulting in a weighted AUC for every temperature to which the samples were exposed (Figure 3B for PVP, Figure 3D for PLGA). In this way it was taken into account that, for example, 1 pixel with an intensity level of 0.002 represents a 10 times smaller amount of that compound compared to a pixel with an intensity of 0.02. Thus, in contrast to the FDPs, these weighted AUC histograms permitted quantitative assessment of the influence of heat upon the microparticle surface. Figure 3B illustrates a clear rise in the amount of PVP present at the sample surface after exposure to heat. Figure 3D shows a complementary overall decrease in the amount of PLGA covering the microsphere surface.

*X-ray Photoelectron Spectroscopy.* Besides ToF-SIMS, XPS was used as a complementary technique in order to

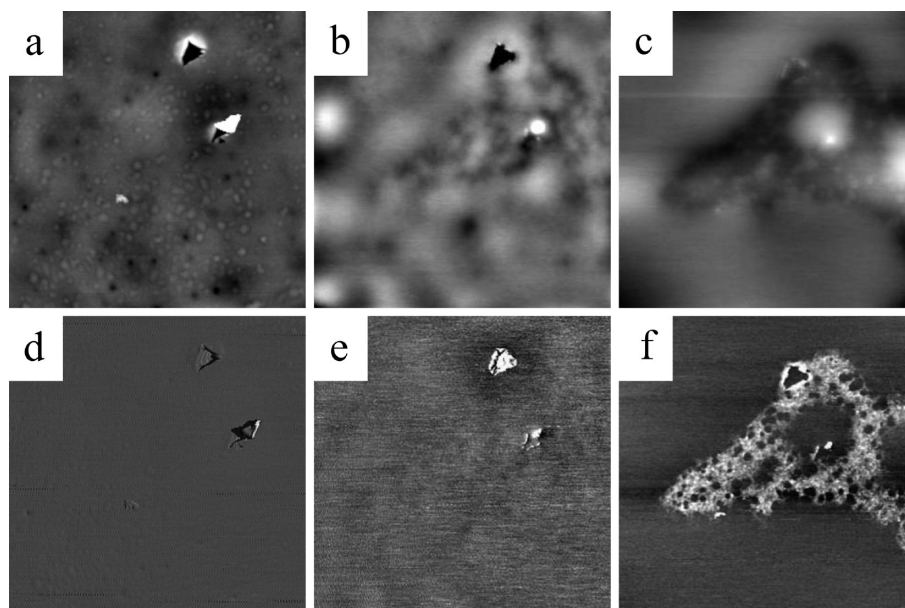


**Figure 5.** Atomic force micrographs of a PLGA/PVP 40/60 wt % sample ( $5 \mu\text{m} \times 5 \mu\text{m}$  scan size). Panels a, b, and c are height images; d, e, and f are the corresponding phase images. Panels a and d are imaged at  $25 \text{ }^\circ\text{C}$ ; b and e at  $45 \text{ }^\circ\text{C}$ ; c and f at  $65 \text{ }^\circ\text{C}$ .

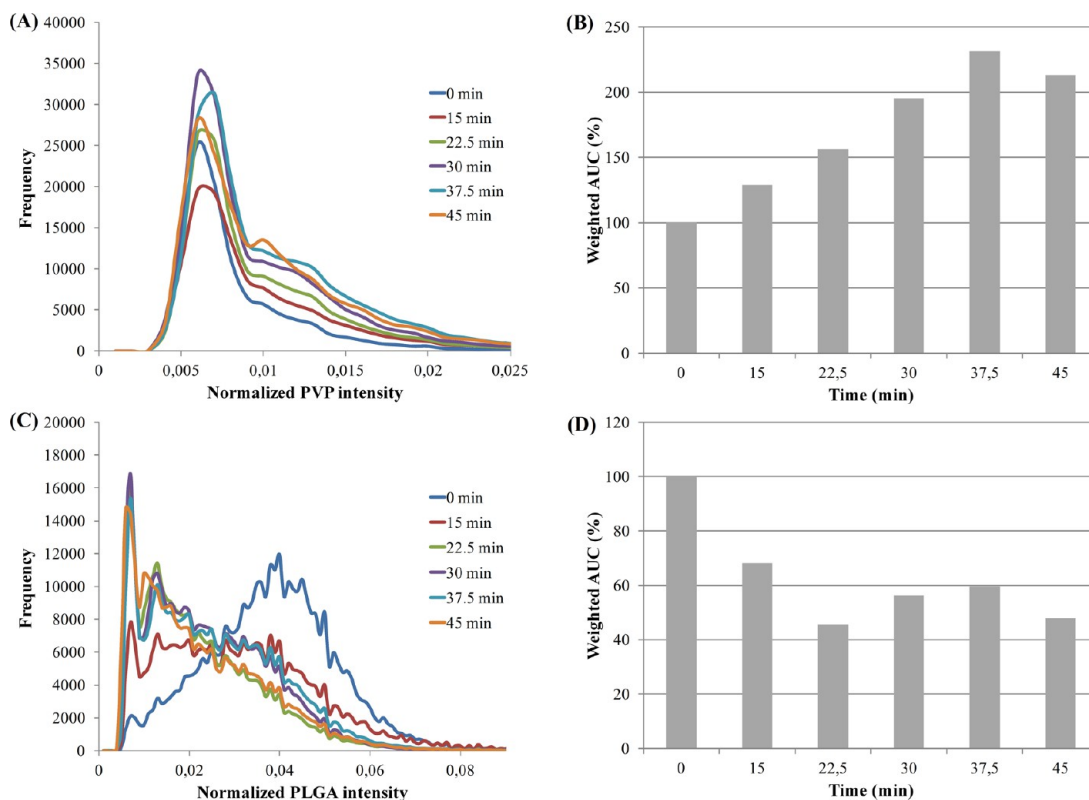


**Figure 6.** ToF-SIMS data. (A) Frequency distribution plot displaying the influence of exposure time to heat upon the presence of PVP at the microsphere surface. (B) Weighted histogram representing the influence of exposure time to heat upon the presence of PVP at the microsphere surface. (C) Frequency distribution plot displaying the influence of exposure time to heat upon the presence of PLGA at the microsphere surface. (D) Weighted histogram representing the influence of exposure time to heat upon the presence of PLGA at the microsphere surface.

investigate how the surface chemically changed when subjected to heat. A PLGA/PVP (40/60 wt %) sample was examined after exposure to  $65 \text{ }^\circ\text{C}$  for 30 min and compared to a reference sample.

When observing the C 1s spectrum for the spray-dried microparticles, the experimental atomic carbon concentration

from the ester bond of PLGA was studied. This functional group was chosen because its peak showed a minimum overlap with other peaks in the C 1s spectrum, which is desired for a correct quantification (Figure 4). A rise or fall of the PLGA content at the surface as a consequence of exposure to an elevated temperature would be characterized by a respective

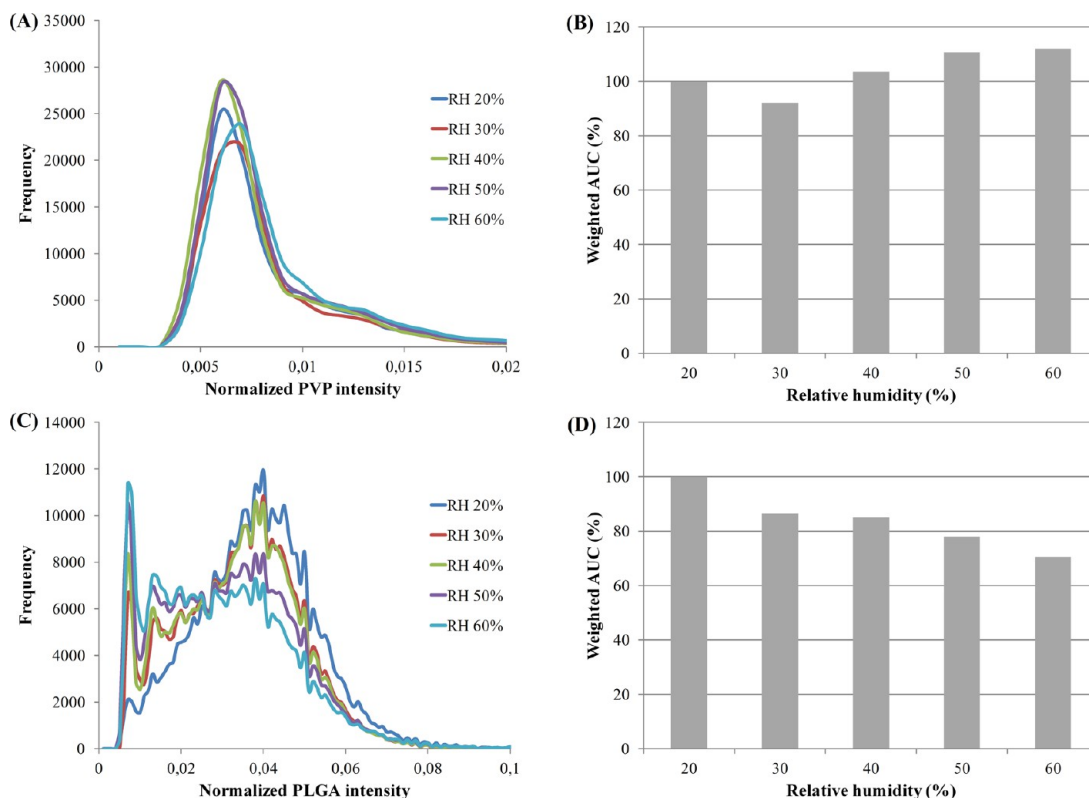


**Figure 7.** ToF-SIMS data. (A) Frequency distribution plot displaying the influence of humidity upon the presence of PVP at the microsphere surface. (B) Weighted histogram representing the influence of humidity upon the presence of PVP at the microsphere surface. (C) Frequency distribution plot displaying the influence of humidity upon the presence of PLGA at the microsphere surface. (D) Weighted histogram representing the influence of humidity upon the presence of PLGA at the microsphere surface.

increase or decrease of the area under the curve (AUC) of this PLGA peak in the C 1s spectrum.

For the reference sample the average AUC was 29.66% (SD 0.91%) of the total amount of carbon present in the sample. After exposure to 65 °C for 30 min, these values evolved to 23.19% with a SD of 5.03%. Despite the increase in SD between the two samples, the diminution in PLGA signal is striking. The larger SD represents most likely the enlarged interparticle differences due to the exposure to heat. SEM was used to study the morphology of the spray-dried microparticles and clearly confirms these interparticle differences (Figure 2).

**2.2. Influence of Heat on the Surface Phase Behavior and Topography.** The influence of elevated temperatures on the topography and the nanoscale surface phase behavior of the spray-dried microparticles was investigated by AFM.

Figure 5 demonstrates the effect of heat on the surface phase behavior of the spray-dried PLGA/PVP sample. The temperature was increased from 25 °C, through 45 °C up to 65 °C (at a RH of maximum 30%), and the same area was imaged for each of these temperatures. When comparing the phase images at each temperature it is clearly observed that upon heating to 65 °C a second phase appears at the particle surface (Figure 5f). The changes observed in this phase image are also reflected in the respective height image (Figure 5c).

**2.3. Influence of Exposure Time to Heat.** To study the influence of the exposure time of the spray-dried samples to heat, the samples were exposed to 65 °C for 15, 22.5, 30, 37.5, and 45 min. ToF-SIMS analysis was performed on these samples with subsequent data analysis. Figure 6A displays the FDP for the PVP signal with an increase in maximum height as

well as increased tailing at the right end of the FDP. The weighted AUC graph (Figure 6B) projects an overall rise in PVP intensity with longer exposure time of the microparticles to heat. It is noticeable that already after 22.5 min of exposure an effect on the particle surface is observed, being an increase in the amount of PVP present.

The FDP for the PLGA signal (Figure 6C) shows a shift to the left-hand side with prolonging exposure time. The weighted AUC graph (Figure 6D) reveals a general lowering in PLGA secondary ion intensity signal with increasing exposure time, compared to the reference sample.

**3. Influence of Humidity.** **3.1. Influence of Humidity on the Chemical Surface Composition. Time-of-Flight Secondary Ion Mass Spectrometry.** In order to investigate the influence of humidity on the surface characteristics of the spray-dried PLGA/PVP samples (40/60 wt %), these were exposed to 30, 40, 50, and 60% relative humidity (RH) for 30 min. Data collection and analysis were performed as described in the Experimental Section.

The results for PVP, after exposure of the sample to elevated humidity, were plotted as a FDP in Figure 7A. It was observed that an increase in humidity resulted in a slight augmentation of the maximum height of the FDP (except for the sample exposed to a RH of 30%) as well as a small shift of this maximum height to the left-hand side. The FDP for PLGA (Figure 7C) revealed a lowering of its original maximum and a shift to the left-hand side combined with an increase in the height of the FDP at that side. The weighted AUC curves showed an augmentation for PVP, except for the sample

exposed to a RH of 30% (Figure 7B) and a general decrease in PLGA with elevated humidity.

**X-ray Photoelectron Spectroscopy.** XPS was also used to investigate how the surface chemically changed upon exposure to humidity. A PLGA/PVP (40/60 wt %) sample was examined after exposure to a RH of 60% for 30 min and compared to a reference sample. Again the experimental atomic carbon concentration from the ester bond of PLGA was studied. The reference sample had an average AUC of 29.66% (SD 0.91%) of the total amount of carbon present. These values evolved to 24.40% with a SD of 7.59% after exposure of the sample to elevated humidity. Despite the increase in SD between the two measurements, the lowering in PLGA signal is considered physically meaningful because the larger SD is most likely due to represent the enlarged interparticle differences resulting from exposure to humidity.

**3.2. Influence of Humidity on the Surface Phase Behavior and Topography.** The influence of humidity on the topography and phase behavior of the spray-dried microparticles was investigated by AFM. Figure 8 displays AFM images before

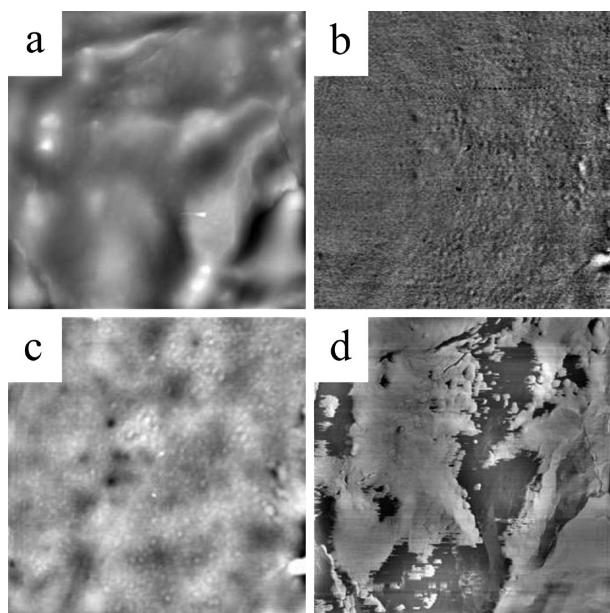


**Figure 8.** Atomic force micrographs of a PLGA/PVP 40/60 wt % sample ( $5 \mu\text{m} \times 5 \mu\text{m}$  scan size). Panels a and c are height images; b and d are the corresponding phase images. Panels a and b are imaged at RH 10%; c and d are obtained after exposure to RH 80%.

and after exposure of the sample to elevated RH. Figures 8a and 8b represent the respective height and phase image of a PLGA/PVP (40/60 wt %) sample recorded at room temperature and 10% RH. Afterward the sample was exposed to a RH of 80% for 30 min. Subsequently the RH was lowered to 10% again, in order to enable imaging of the particle surface (Figure 8c,d). It is observed that elevated humidity affects the composition of the particle surface with the appearance of an additional phase at the particle surface. This effect is irreversible (within the time frame of the experiment) when decreasing the humidity again.

Figure 9 shows a PLGA/PVP 20/80 wt % sample, where a change in pore size is observed due to elevated humidity. First, a fine network with small pores is imaged at a RH of 20% (Figures 9a and 9c). After increasing the humidity up to 60%, less well-defined and larger pores are observed as well as a drop

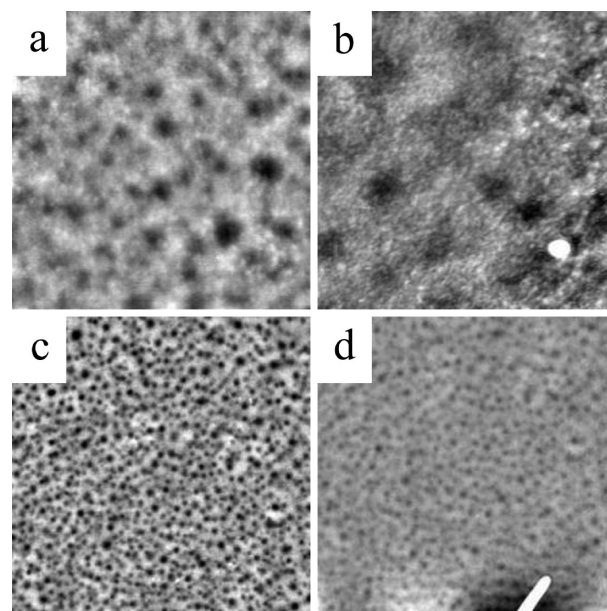


**Figure 9.** AFM height images of a PLGA/PVP (20/80 wt %) sample. Panels a and c are imaged at RH 20%; b and d are the same areas imaged at RH 60% (a and b,  $1.8 \times 1.8 \mu\text{m}^2$  scan size; c and d,  $4 \times 4 \mu\text{m}^2$  scan size).

in the number of pores present at the surface (Figures 9b and 9d).

**3.3. Influence of Exposure Time on Humidity.** Samples were exposed to 60% RH for 15, 22.5, 30, 37.5, and 45 min in order to investigate the influence of exposure time to humidity upon the sample surface. ToF-SIMS analysis was performed on these samples. Figure 10A displays the FDP obtained for the PVP signal. A clear tendency with prolonged exposure time could not be observed for the intensity signal originating from PVP. The weighted AUC histogram (Figure 10B) only shows a prominent increase in PVP intensity for the sample with the longest exposure time (45 min). The FDP obtained from the PLGA signal (Figure 10C) is characterized by a shift to the left-hand side for samples with an increasing exposure time. The weighted AUC curve reveals a decrease in PLGA intensity for exposure times over 15 min.

## DISCUSSION

Extensive research has already been carried out to prove the influence of both heat and humidity on bulk characteristics of pharmaceutical formulations.<sup>2–10</sup> The novelty of this study lies in the conception of the formulation surface as a determining and even predicting factor for the bulk characteristics of that formulation. Furthermore a powerful combination of state-of-the-art techniques allowing nanoscale surface characterization was successfully applied.

For the reference sample, MDSC was used to study the phase behavior before exposure of the sample to heat or humidity. Figure 1A shows the mixing  $T_g$ s in the thermograms, which indicate the presence of two mixed amorphous phases: a PLGA-rich phase containing some PVP and a PVP-rich phase containing some PLGA. The amount of PVP present in the PLGA-rich phase and the amount of PLGA present in the PVP layer was estimated from the observed  $T_g$ s using the Gordon–Taylor equation. The results demonstrate that the PLGA-rich phase contains 15% PVP and the PVP-rich phase comprises 3%

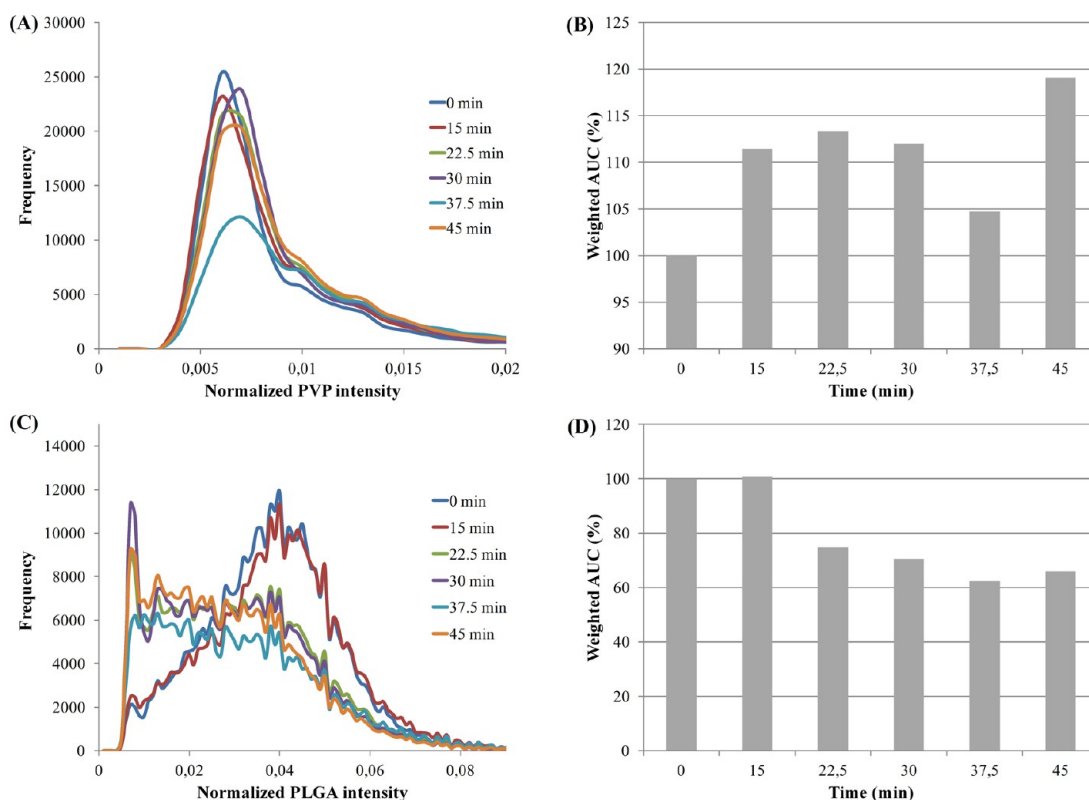


**Figure 10.** ToF-SIMS data. (A) Frequency distribution plot displaying the influence of exposure time to humidity upon the presence of PVP at the microsphere surface. (B) Weighted histogram representing the influence of exposure time to humidity upon the presence of PVP at the microsphere surface. (C) Frequency distribution plot displaying the influence of exposure time to humidity upon the presence of PLGA at the microsphere surface. (D) Weighted histogram representing the influence of exposure time to humidity upon the presence of PLGA at the microsphere surface.

PLGA. The phase behavior of this reference sample was then compared to that of samples exposed to heat or humidity.

**Influence of Heat.** The first part of this study focused on the influence of exposure to heat upon the phase behavior of the spray-dried polymeric matrix both at the bulk level (investigated by MDSC) and at the surface level (examined by ToF-SIMS, XPS, and AFM).

MDSC results demonstrated that exposure of the sample to heat influenced the  $T_g$  of the spray-dried polymeric matrix in terms of its value (Figure 1B) as well as the width of the  $T_g$  region (Figure 1C). Thus, MDSC showed a change in the bulk miscibility and hence phase behavior of the spray-dried microspheres.

In addition, surface analysis revealed an undeniable influence of heat upon the surface characteristics of the polymeric microspheres, and more specifically upon their chemical composition, phase behavior, and topography. The conclusion for all techniques used (ToF-SIMS, XPS, and AFM) was that exposure of the spray-dried polymeric matrix to elevated temperatures resulted in a surface rearrangement with the appearance of spots of the underlying PVP layer at the PLGA surface. The overall result is an augmented surface coverage of PVP combined with a lower PLGA coverage.

The ToF-SIMS results displayed in Figure 3a demonstrate that there is a tendency for the respective FDP to show an increased maximum height as well as tailing at the right-hand side for the PVP secondary ion intensity upon exposure of the samples to elevated temperature. The rise in maximum height represents an augmentation in the number of pixels and hence the number of  $6.67 \mu\text{m} \times 6.67 \mu\text{m}$  sized areas with that specific

intensity level. This suggests an increased surface coverage by PVP at the sample surface after exposure to elevated temperature. The shift to the right-hand side of the FDP indicates an augmentation in the number of PVP spots with a high intensity level, suggesting a high amount of PVP. These two observations imply that, upon exposure of the sample to heat, there is an increase in PVP at the surface, caused by both a rise in the area covered by PVP at the surface and an augmentation of the average amount of PVP present at these spots.

The shift to the left-hand side of the FDP for PLGA represents an increase in the number of PLGA spots with a low intensity level and hence an augmentation in surface spots with a lower amount of PLGA present. This indicates a general decrease in the amount of PLGA present at the sample surface after exposure to heat and is complementary to the observations for PVP.

The histograms representing the weighted AUC not only portray the increase or decrease in the number of spots present at the surface but also include the rise or lowering of the intensity level measured. Hence, these graphs represent the total amount of compound present at the sample surface. These graphs show that the result was a general augmentation of the weighted AUC for PVP (Figure 3b) and thus an increase in the total amount of PVP present at the sample surface. The opposite was observed for PLGA: a decrease in the weighted AUC, representing a decrease in the total amount of PLGA present at the sample surface and hence a lower surface coverage of PLGA (Figure 3d).

XPS experiments revealed a decrease in PLGA present at the sample surface upon exposure of the samples to elevated temperatures. The significant increase in variability observed by XPS measurements indicates a rise in the sample heterogeneity caused by the raised temperature treatment. This originates from the fact that exposure to heat enlarges the interparticle differences caused by cracks and other surface damage which are mainly caused by particle–particle and particle–wall collisions during the spray drying process, and particle rupture due to solvent evaporation. SEM images (Figure 2) portray these interparticle differences and hence support our conclusion. In those cases of surface damage, it is not the original PLGA surface layer but rather the underlying PVP layer that is exposed at the particle surface and will hence be detected. Upon exposure of the sample to heat, it is clear that the PVP layer directly exposed to these elevated temperatures will react differently than the intact PLGA surface layer. This results in an accelerated augmentation of PVP present at the sample surface because of more direct access to the PVP layer. Hence an increase in sample heterogeneity and thus variability can be observed.

Another method used to study the consequences of exposure to heat upon the sample surface was AFM. This technique showed the influence of heat with the appearance of a second phase at the particle surface when the sample was heated up to 65 °C. Combining the AFM results with the preceding ToF-SIMS and XPS results leads to the conclusion that this second phase was PVP appearing at the surface.

The influence of prolonged exposure of the samples to elevated temperature was investigated by means of ToF-SIMS. The increase in maximum height as well as increased tailing at the right end of the FDP for the PVP ion intensity (Figure 6A) indicate an augmentation both of the number of spots covered with PVP and of the amount of PVP present at these particular surface spots. The weighted AUC histogram (Figure 6B) shows a clear rise in the intensity signal coming from PVP and thus in the total amount of PVP present at the microparticle surface with longer exposure time.

For PLGA the shift to the left-hand side of the FDP (Figure 6C) and the decrease in the weighted AUC graph (Figure 6D) with prolonged exposure indicate a drop in the amount of PLGA present at the particle surface, though this tendency is less pronounced than that of the increase in PVP.

At these time points, the changes are observable at the nanoscale and at the sample surface and possibly do not yet have a significant influence on the bulk characteristics of the formulation (such as bulk miscibility and release behavior). Nevertheless, these findings indicate that exposure of the samples to heat has an influence on the sample characteristics. This implies that prolonged exposure over time might influence the bulk miscibility and release behavior of future formulations. Hence these observations provide an insight into the response of the spray-dried polymeric matrix to heat and help to elucidate the expected stability and dissolution behavior of the formulation. It will facilitate the development of a drug matrix with desired and tunable characteristics in terms of physicochemical stability and drug release profile in a later stage of research.

**Influence of Humidity.** The second part of this study investigated the effect of exposure to humidity upon the phase behavior of the spray-dried polymeric matrix, again both at the bulk level and at the surface level. The observations for

exposing the microspheres to humidity were similar to those for exposure of the samples to heat.

MDSC results demonstrated again that exposure of the sample to humidity influenced the  $T_g$  of the spray-dried microspheres in terms of its value (Figure 1D) as well as the width of the  $T_g$  range (Figure 1E). This implies that there is a change in the bulk miscibility and hence phase behavior of spray-dried samples upon exposure to humidity.

As for exposure to heat, surface analysis revealed a clear influence of humidity upon the surface characteristics of the polymeric microspheres leading toward the same conclusion: exposure of the spray-dried polymeric matrix to elevated humidity resulted in an augmented surface coverage of PVP combined with a lower PLGA coverage.

ToF-SIMS was used to study the presence of PVP at the particle surface when exposed to elevated humidity. The increase in AUC of the FDP represents an augmentation of PVP at the sample surface, as humidity rises (Figure 7A). Not only is there an increased number of PVP regions present at the surface but also the augmented amount of PVP present at each pixel is taken into account in the weighted AUC histogram (Figure 7B). The result is an increased surface coverage of PVP. The evolution of the presence of PLGA at the microparticle surface with increasing humidity was mapped in Figures 7C and 7D. The peak rising at the left-hand side of the FDP (Figure 7C) with elevated humidity represents the increase in surface regions covered with a lower amount of PLGA and hence a lower total surface coverage by PLGA. This overall decrease of PLGA is confirmed in Figure 7D.

Upon exposure of the samples to elevated humidity, XPS experiments showed a decrease of PLGA present at the sample surface, which confirms the results of the ToF-SIMS study. As for the samples exposed to heat, a significant increase in variability was observed, indicating an increase in the sample heterogeneity.

The influence of humidity upon the sample surface observed by AFM is depicted in Figure 8: exposure of the surface to elevated humidity results in the appearance of a second phase at the particle surface. The preceding ToF-SIMS and XPS results already revealed that it is in fact the underlying PVP layer that appears at the PLGA surface of the microspheres.

The study concerning the influence of the exposure time to humidity revealed that prolonged exposure resulted in a rise in the amount of PVP present at the sample surface. When taking into account the weighted AUC, this influence was already noticeable after 15 min of exposure (Figure 10B). For PLGA the shift to the left-hand side of the FDP indicated again an increase in the number of spots with a reduced PLGA intensity (and hence a lower PLGA surface coverage) and a lowering of the number of spots with a high PLGA content (Figure 10C). The weighted AUC histogram (Figure 10D) revealed that the effect already became observable after 22.5 min of exposure. Overall, the effect was less pronounced compared to the prolonged exposure to elevated temperature for the selected parameters.

**Proposed Mechanism.** After observing that exposure of the spray-dried microspheres to heat and humidity had an influence on the sample surface, a hypothesis was constructed, suggesting the cause of this surface rearrangement at the molecular level. For both heat and humidity the origin of the surface rearrangement is hypothesized to be dual.

The first and most determinative cause of the surface reorganization observed is proposed to be found in the large

difference in  $T_g$  between the two polymers used, being ca. 38 °C for PLGA and ca. 172 °C for PVP (Figure 1A). The  $T_g$  can generally be seen as a straightforward parameter for comparing the molecular mobility of different compounds at a given temperature. This is because the  $T_g$  is the transition temperature between the glassy, solid-like state where molecular mobility is low and relaxation times are usually high and the rubbery, liquid-like state, where the opposite is true. When the temperature is lower than the  $T_g$ , the sample will have a limited molecular mobility compared to above the  $T_g$ . The large difference in  $T_g$  between both polymers will hence be translated into significant differences in molecular mobility of these two components at temperatures between the two  $T_g$ 's.<sup>14,15</sup>

The exposure of the sample to heat will hence predominantly influence the molecular mobility of PLGA because of its low  $T_g$  compared to PVP. When subjected to heat, there will be a transfer from the glassy PLGA phase into or further into the undercooled liquid state with an increased molecular mobility.

Analogously, the exposure of the sample to humidity also results in elevated molecular mobility of (predominantly) the PLGA phase. This can be related to the plasticizing effect of the rising amount of water present in the environment. The plasticizing and potentially destabilizing effect of water on PLGA has already been reported.<sup>16</sup> Due to the low  $T_g$  of water (reported from  $-137$  to  $-108$  °C<sup>15</sup>) even the presence of a minor amount of water can significantly lower the  $T_g$  of the PLGA phase (based upon the Gordon–Taylor equation) and hence result in an increased molecular mobility at a given temperature.

Thus exposure of the sample both to heat and to humidity is hypothesized to increase the molecular mobility of PLGA relative to PVP. This rise in molecular mobility will allow the surface reorganization observed by ToF-SIMS, XPS, and AFM.

Because the  $T_g$  is a measure for the molecular mobility of a compound at a given temperature, it can be stated that the influence of heat and humidity on the surface of the spray-dried polymers is largely dependent upon the thermal characteristics of the polymers used, and hence this approach could be generalized and applied to other polymers as well.

For example, the AFM images in Figure 5 depict that only after exposure of the sample to 65 °C, a temperature well above the  $T_g$  of PLGA, surface rearrangement occurs within the time frame studied.

Combined with the rise in molecular mobility of PLGA, the second cause for the observed microparticle surface rearrangement is suggested to be the relative swelling of PVP.

It is generally known that PVP swells when it is exposed to humidity. To support this statement thermogravimetric analysis (TGA) was performed to determine the uptake of water for both polymers (PLGA and PVP) when exposed to increased humidity. Spray-dried PLGA and PVP reference samples were exposed to RH 60% for three hours. Results are displayed in Figure 1 of the Supporting Information. This experiment clearly indicates that the hydrophilic PVP takes up water to a much higher extent: 5.36% water uptake for PVP compared to 0.67% for PLGA, representing an 8-fold higher water absorption for PVP. Presumably the absorbed water will be situated between the polymer chains and hence result in significant swelling of PVP compared to PLGA. Combined with the increased molecular mobility for PLGA, this might lead to the appearance of spots of PVP at the PLGA surface layer.

The observed increase in pore size (Figure 9) with increased relative humidity can thus be explained by the swelling of PVP as a consequence of the humidity, resulting in a physical rearrangement of the surface and the loss of the fine matrix network with accompanying pores.

Swelling of PVP due to exposure to heat is not observed or reported yet, but, if present, is expected to be less significant than swelling of PVP due to humidity. This because of the high  $T_g$  of this polymer and the fact that substantial swelling is only expected around the polymer's glass transition.

In summary, the appearance of the underlying PVP layer at the PLGA surface of the microspheres is proposed to be mainly caused by the increased molecular mobility of the PLGA surface layer, to a lesser extent combined with the swelling behavior of PVP upon exposure to humidity or heat.

## CONCLUSIONS

The surface characteristics (chemical composition, phase behavior, and topography) of spray-dried PVP/PLGA microspheres are affected by exposure to heat and humidity. When exposed to these conditions a rearrangement occurs whereby a decrease in PLGA present at the surface is observed, coupled with an increase in PVP. This phenomenon could be explained based upon the relative thermal characteristics and consequent molecular mobility of the two polymers as well as the known swelling behavior of PVP.

This study provides us with guidelines concerning the storage of future formulations based upon this polymeric matrix: both temperature and humidity should be controlled, with a smaller tolerance level for the temperature to which the samples are exposed.

Furthermore it implies that exposure to elevated temperatures and humidity might influence the bulk miscibility and release behavior of future formulations.

## ASSOCIATED CONTENT

### Supporting Information

Figure depicting TGA analysis to determine the water uptake for PLGA and PVP. This material is available free of charge via the Internet at <http://pubs.acs.org>.

## AUTHOR INFORMATION

### Corresponding Author

\*E-mail: [guy.vandenmooter@pharm.kuleuven.be](mailto:guy.vandenmooter@pharm.kuleuven.be).

### Notes

The authors declare no competing financial interest.

## ACKNOWLEDGMENTS

E. F. Smith and V. Ciarnelli are gratefully acknowledged for performing the XPS experiments. P. Rombaut is thanked for his general technical support. FWO-Vlaanderen is acknowledged for financial support (G.0486.10N).

## REFERENCES

- (1) Meeus, J.; Chen, X.; Scurr, D. J.; Ciarnelli, V.; Amssoms, K.; Roberts, C. J.; Davies, M. C.; Van den Mooter, G. Nanoscale surface characterization and miscibility study of a spray-dried injectable polymeric matrix consisting of poly(lactic-co-glycolic acid) and polyvinylpyrrolidone. *J. Pharm. Sci.* **2012**, *101*, 347–385.
- (2) Greco, S.; Authelin, J. R.; Leveder, C.; Segalini, A. A practical method to predict physical stability of amorphous solid dispersions. *Pharm. Res.* **2012**, *10*, 2792–805.

(3) Jondhale, S.; Bhise, S.; Pore, Y. Physicochemical investigations and stability studies of amorphous gliclazide. *AAPS PharmSciTech* **2012**, *13*, 448–459.

(4) Sato, H.; Kawabata, Y.; Yuminoki, K.; Hashimoto, N.; Yamauchi, Y.; Ogawa, K.; Mizumoto, T.; Yamada, S.; Onoue, S. Comparative studies on physicochemical stability of cyclosporine A-loaded amorphous solid dispersions. *Int. J. Pharm.* **2012**, *426*, 302–306.

(5) Bley, H.; Fussnegger, B.; Bodmeier, R. Characterization and stability of solid dispersions based on PEG/polymer blends. *Int. J. Pharm.* **2010**, *390*, 165–173.

(6) Ghebremeskel, A. N.; Vemavarapu, C.; Lodaya, M. Use of surfactants as plasticizers in preparing solid dispersions of poorly soluble API: stability testing of selected solid dispersions. *Pharm. Res.* **2006**, *23*, 1928–1936.

(7) Rumondor, A. C. F.; Stanford, L. A.; Taylor, L. S. Effects of polymer type and storage relative humidity on the kinetics of felodipine crystallization from amorphous solid dispersions. *Pharm. Res.* **2009**, *26*, 2599–2606.

(8) Rumondor, A. C. F.; Wilström, H.; Van Eerdenbrugh, B.; Taylor, L. S. Understanding the tendency of amorphous solid dispersions to undergo amorphous-amorphous phase separation in the presence of absorbed moisture. *AAPS PharmSciTech* **2011**, *12*, 1209–1219.

(9) Marsac, P. J.; Rumondor, A. C. F.; Nivens, D. E.; Kestur, U. S.; Stanciu, L.; Taylor, L. S. Effect of temperature and moisture on the miscibility of amorphous dispersions of felodipine and poly(vinyl pyrrolidone). *J. Pharm. Sci.* **2010**, *99*, 169–185.

(10) Rumondor, A. C. F.; Marsac, P. J.; Stanford, L. A.; Taylor, L. S. Phase behaviour of poly(vinylpyrrolidone) containing amorphous solid dispersions in the presence of moisture. *Mol. Pharmaceutics* **2009**, *6*, 1492–1505.

(11) Pikal, M. J.; Chang, L.; Tang, X. Evaluation of glassy-state dynamics from the width of the glass transition: results from theoretical simulation of differential scanning calorimetry and comparisons with experiment. *J. Pharm. Sci.* **2004**, *93*, 981–994.

(12) Brüning, R.; Sutton, M. Fragility of glass-forming systems and the width of the glass transition. *J. Non-Cryst. Solids* **1996**, *205–207*, 480–484.

(13) Savin, D. A.; Larson, A. M.; Lodge, T. P. Effect of the composition on the width of the calorimetric glass transition in polymer-solvent and solvent-solvent mixtures. *J. Polym. Sci., Part B: Polym. Phys.* **2004**, *42*, 1155–1163.

(14) Janssens, S.; Van den Mooter, G. Physical chemistry of solid dispersions. *J. Pharm. Pharmacol.* **2009**, *61*, 1571–1586.

(15) Baird, J. A.; Taylor, L. S. Evaluation of amorphous solid dispersion properties using thermal analysis techniques. *Adv. Drug Delivery Rev.* **2012**, *64*, 396–421.

(16) Blasi, P.; D'Souza, S. S.; Selmin, F.; DeLuca, P. P. Plasticizing effect of water on poly(lactide-co-glycolide). *J. Controlled Release* **2005**, *108*, 1–9.